

RESEARCH ARTICLE

# Fabrication of an *in vitro* three-dimensional tumor model using liver-derived decellularized extracellular matrix/gelatin methacrylate bioink for investigating cancer characteristics and drug resistance

## Supplementary file

The infrared spectra of gelatin and GelMA, as shown in **Figure S1A**, were mainly composed of amide groups (bands A, I, II, and III). As shown in **Figure S1B**, the absorption peak at  $3318\text{ cm}^{-1}$  is attributed to the amide A band, and the peak at  $3075\text{ cm}^{-1}$  corresponds to the amide B band, both of which are primarily caused by N–H stretching vibrations. The amide I band, located around  $1654\text{ cm}^{-1}$ , is associated with C=O stretching vibrations, while the amide II band at  $1542\text{ cm}^{-1}$  is attributed to the coupling of N–H bending vibration and C–N stretching vibrations. The characteristic amide peaks of GelMA, particularly the amide I and II bands, were significantly enhanced, indicating the formation of new amide bonds as a result of the reaction between gelatin and methyl methacrylate. This confirms the successful introduction of methacrylamide groups onto the gelatin molecule chain.

**Figure S1C** displays the thermogravimetric curves of GelMA and gelatin, showing that both materials underwent three stages of weight loss between 5 and  $500^\circ\text{C}$ . The weight loss at the first decomposition stage observed from 0 to  $160^\circ\text{C}$  can be attributed to the evaporation of free water, while the loss between 30 and  $260^\circ\text{C}$  is likely due to protein degradation at elevated temperatures. Across the entire temperature range, the final weight loss of gelatin was slightly lower than that of GelMA. However, GelMA exhibited slower weight loss than gelatin between  $100$  and  $250^\circ\text{C}$ , possibly due to increased molecular and intermolecular hydrogen bonding resulting from the GelMA modification.

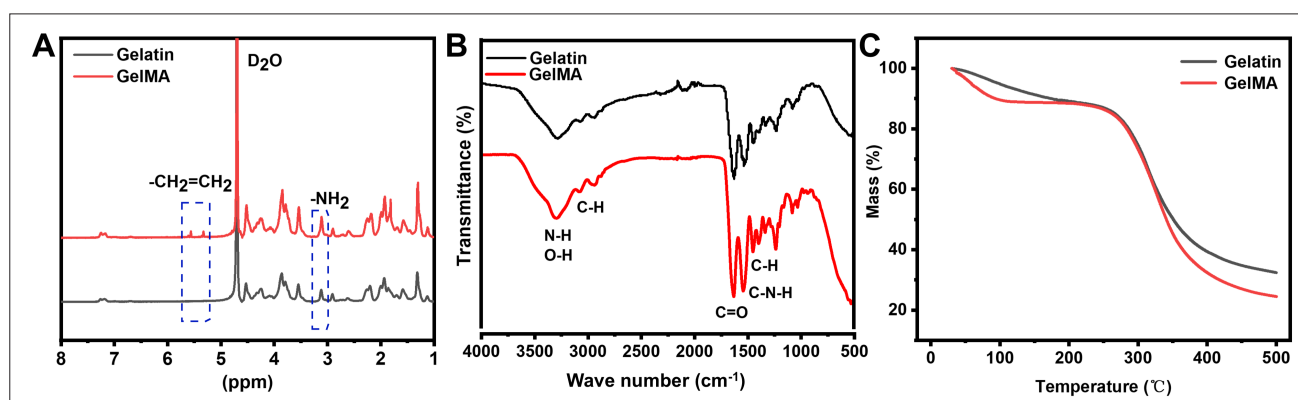


**Figure S1.** Analysis of gelatin methacrylate (GelMA). (A) Proton nuclear magnetic resonance of GelMA. (B) Fourier-transform infrared spectra of GelMA. (C) Thermal gravimetric analysis curves of GelMA.

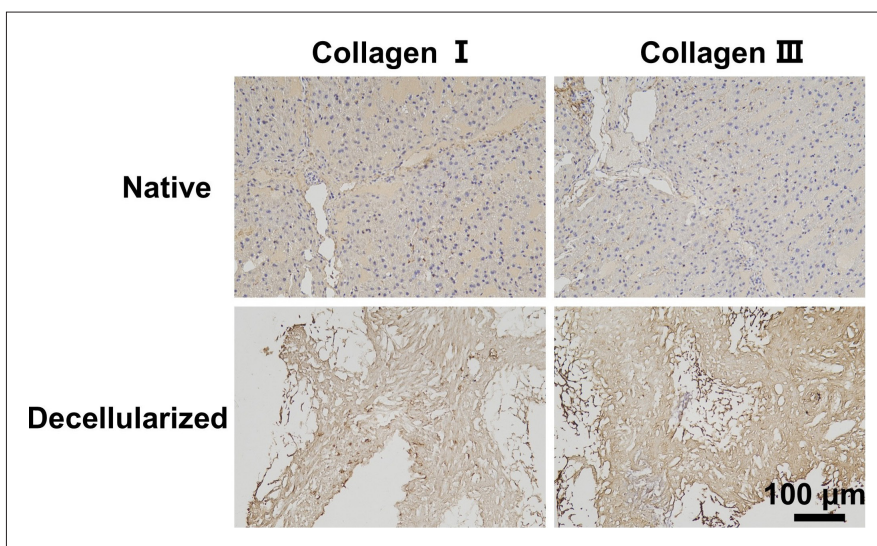


Figure S2. Staining of collagen I and III. Scale bar: 100 μm; magnification = 40×.

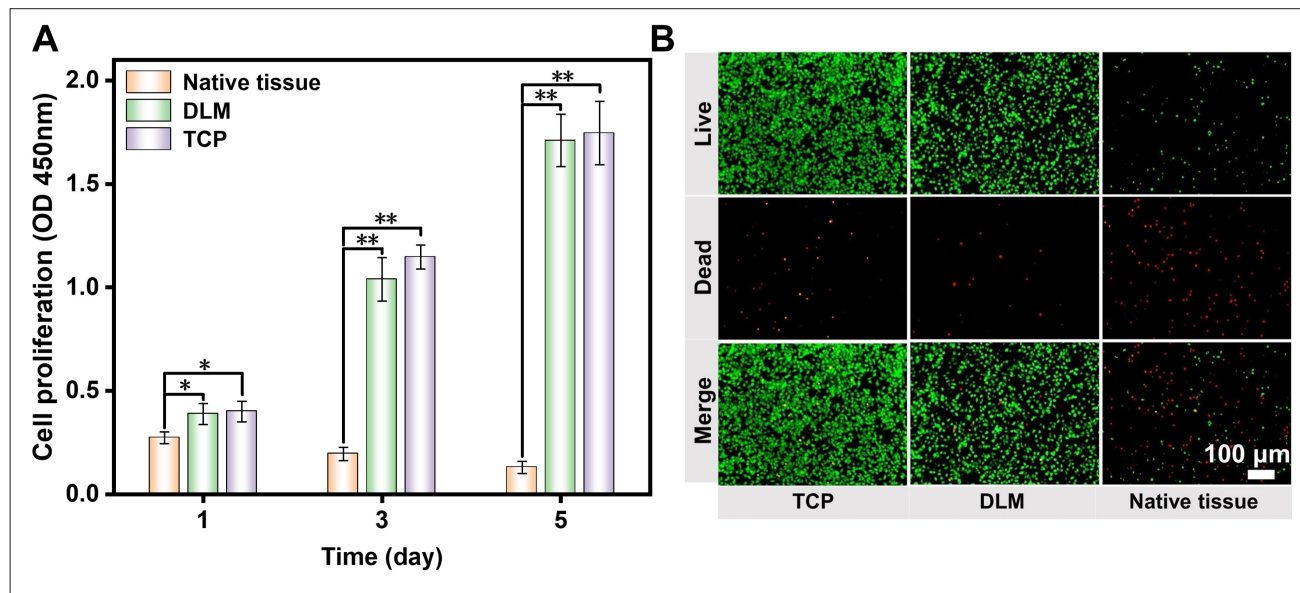
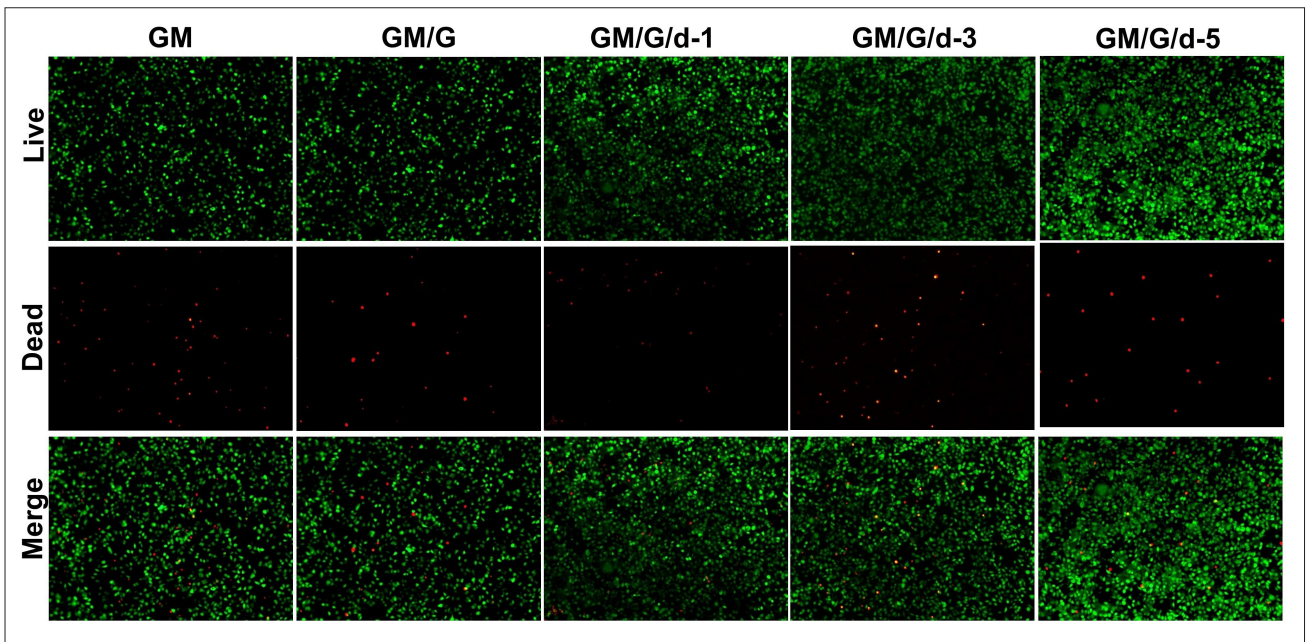
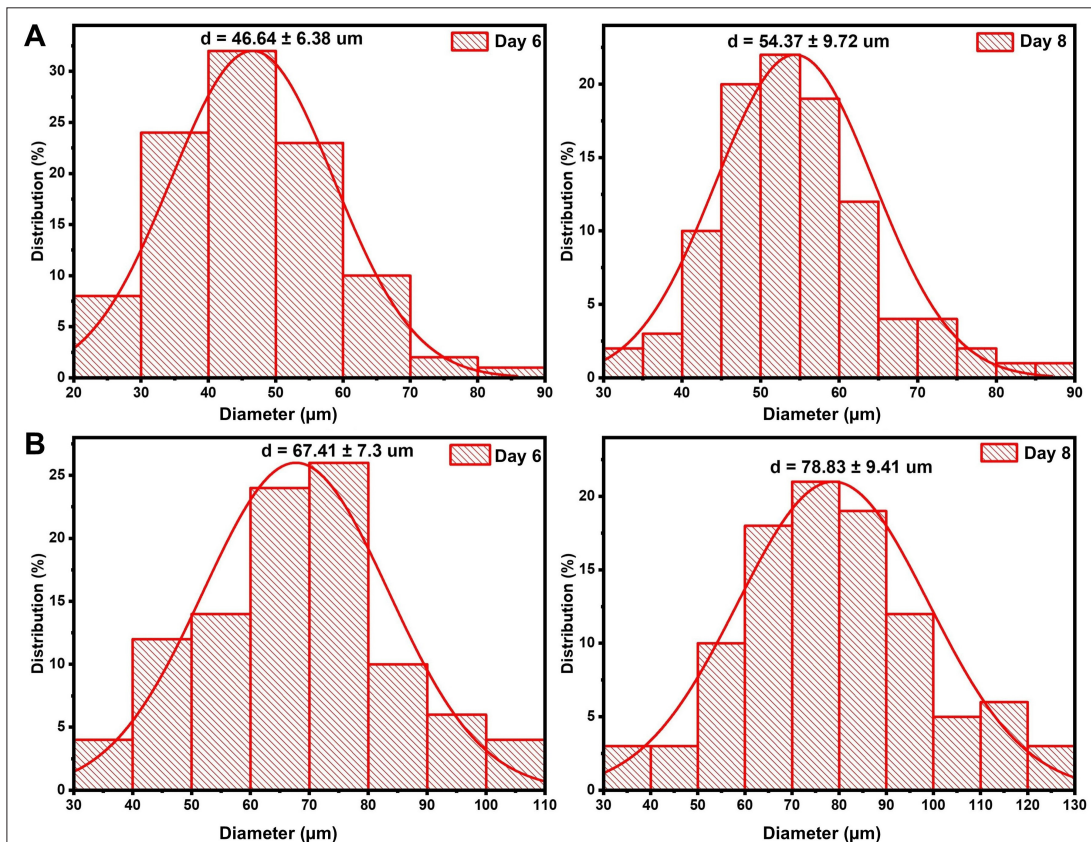


Figure S3. Determination of cell cytotoxicity. (A) Optical density (OD) values of native tissue and decellularized liver matrix (DLM). (B) Live/dead staining of L929 cells in native tissues and DLM extracts. Scale bar: 100 μm; magnification = 20×. \*  $p < 0.05$ , \*\*  $p < 0.01$ . Abbreviation: TCP, tissue culture plate.



**Figure S4.** Cell cytotoxicity of five different scaffolds: GM, GM/G, GM/G/d-1, GM/G/d-3, and GM/G/d-5. Scale bar: 200  $\mu\text{m}$ ; magnification = 20 $\times$ . Notes: GM: 10% (w/v) gelatin methacrylate (GelMA); GM/G: 10% (w/v) GelMA and 5% (w/v) gelatin; GM/G/d-1, GM/G/d-3, and GM/G/d-5: GM/G combined with decellularized extracellular matrix at concentrations of 1%, 3%, and 5% (w/v), respectively.



**Figure S5.** Distribution of spheroid diameters in three-dimensional constructs on days 6 and 8: (A) without and (B) with the addition of decellularized extracellular matrix.

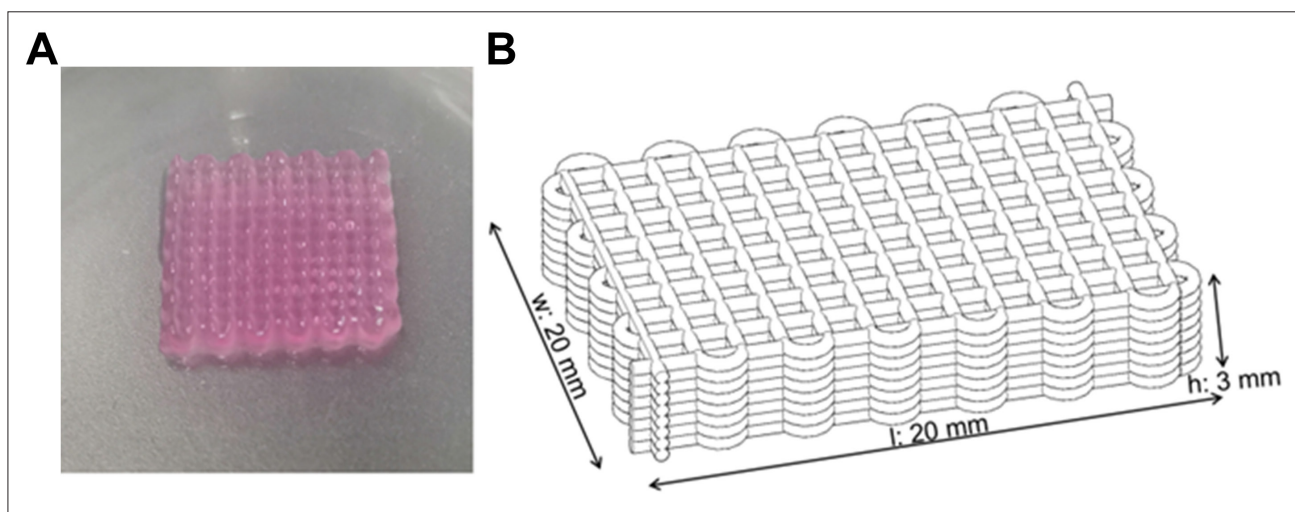


**Figure S6.** Three-dimensional bioprinted hydrogel scaffolds used in this study. (A) Photograph of the three-dimensional bioprinted hydrogel scaffolds used for constructing the *in vitro* liver cancer model. (B) Schematic illustration of the scaffold's layered grid structure, with dimensions of 20 mm × 20 mm × 3 mm (length × width × height).

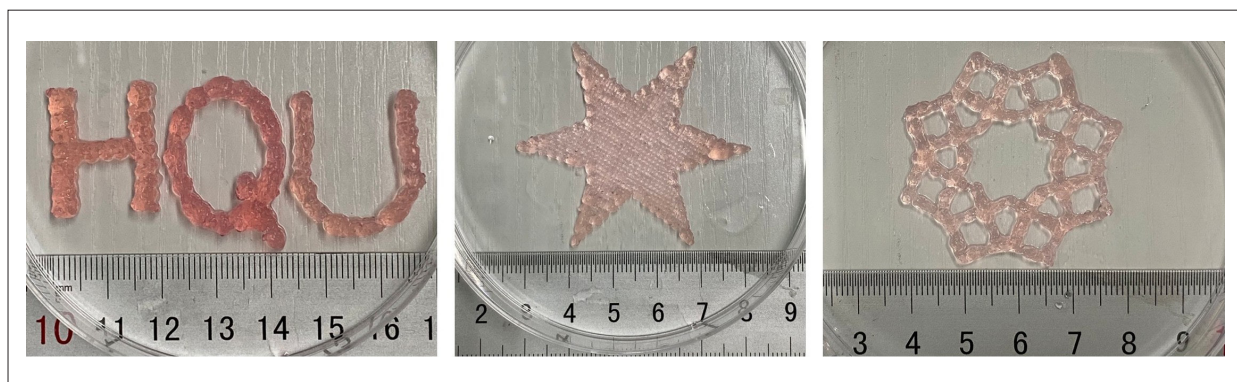


**Figure S7.** Representative three-dimensional printed complex structures using the GM/G/d-5 bioink, including stylized letters (“HQU”), a six-pointed star, and a flower-like biomimetic mesh. Note: GM/G/d-5 consists of 10% (w/v) gelatin methacrylate and 5% (w/v) gelatin combined with decellularized extracellular matrix at a concentration of 5% (w/v).

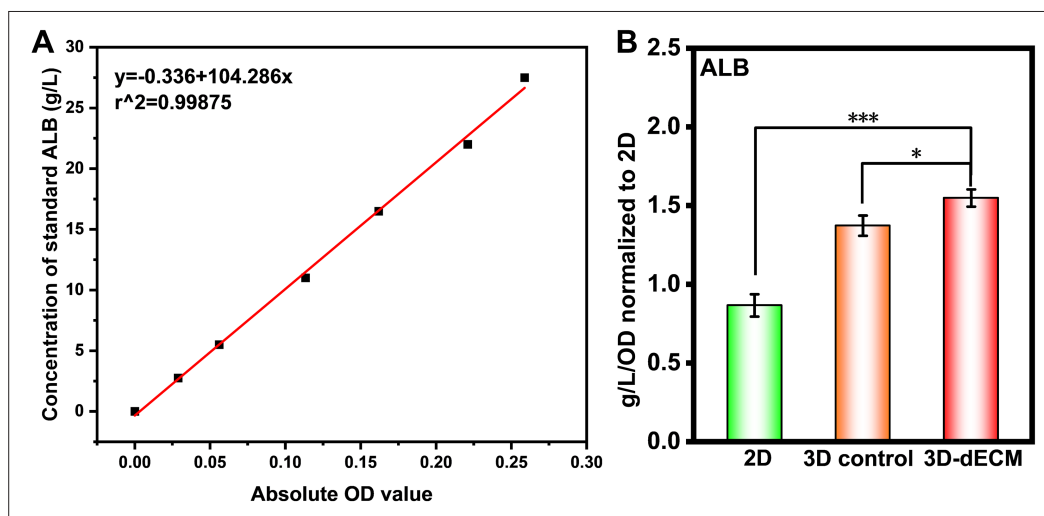


**Figure S8.** Standard calibration curve for albumin (ALB) concentration. \*  $p < 0.05$ , \*\*\*  $p < 0.001$ . Abbreviations: dECM, decellularized extracellular matrix; OD, optical density; 2D, two-dimensional; 3D, three-dimensional.

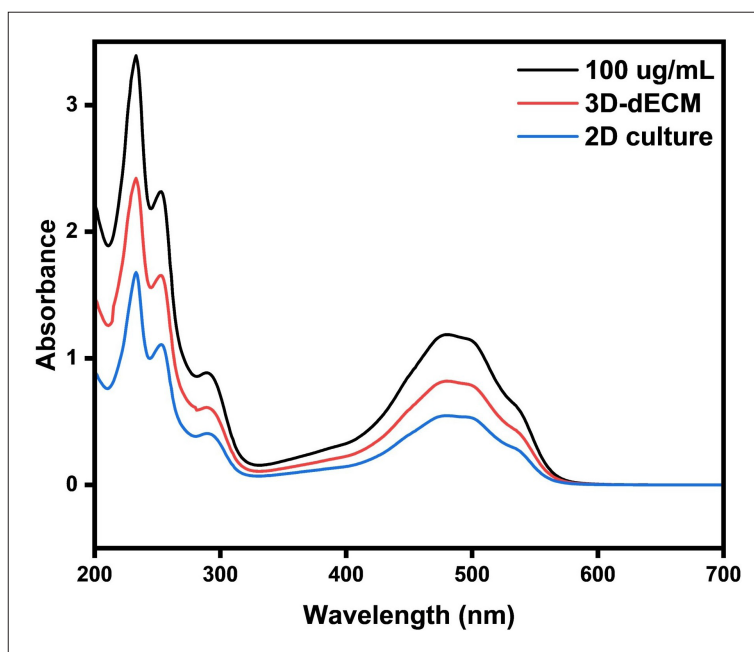


**Figure S9.** Ultraviolet-visible absorption spectra of doxorubicin (DOX) after 12 h of incubation with two-dimensional (2D) culture and three-dimensional (3D)-decellularized extracellular matrix (dECM) constructs. The black line represents the initial DOX solution (100  $\mu\text{g/mL}$ ), while the red and blue lines correspond to the residual DOX in the 3D-dECM and 2D culture groups, respectively.